The Journal of Infectious Diseases

MAJOR ARTICLE

Characterisation of the spatio-temporal localisation of a pan-Mucorales specific antigen during germination and immunohistochemistry

Alyssa C. Hudson[1,2], Dora E. Corzo-León[1], Iana Kalinina[1], Duncan Wilson[1], Christopher R. Thornton[3,4], Adilia Warris[1], Elizabeth R. Ballou[1*]

1) Medical Research Council Centre for Medical Mycology at the University of Exeter, Exeter, UK; 2) Royal Devon University Hospitals NHS Foundation Trust, Exeter, UK; 3) Biosciences, Faculty of Health and Life Sciences, University of Exeter, Exeter, UK; 4) ISCA Diagnostics Ltd., Hatherly Laboratories, Exeter, UK

Background*:** Mucormycosis is an aggressive, invasive fungal infection caused by moulds in the order Mucorales. Early diagnosis is key to improving patient prognosis, yet relies on insensitive culture or non-specific histopathology. A pan-Mucorales specific monoclonal antibody (mAb), TG11, was recently developed. Here, we investigate the spatio-temporal localisation of the antigen and specificity of the mAb for immunohistochemistry. ***Methods: We use immunofluorescence (IF) microscopy to assess antigen localisation in eleven Mucorales species of clinical importance and live imaging of *Rhizopus arrhizus* germination. Immunogold transmission electron microscopy (immunoTEM) reveals the sub-cellular location of mAb TG11 binding. Finally, we perform immunohistochemistry of *R. arrhizus* in an *ex vivo* murine lung infection model alongside lung infection by *Aspergillus fumigatus*. ***Results*:** IF revealed TG11 antigen production at the emerging hyphal tip and along the length of growing hyphae in all Mucorales except *Sakasenea*. Timelapse imaging revealed early antigen exposure during spore germination and along the growing hypha. ImmunoTEM confirmed mAb TG11 binding to the hyphal cell wall only. The TG11 mAb specifically stained Mucorales but not *Aspergillus* hyphae in infected murine lung tissue. **Conclusions:** TG11 detects early hyphal growth and has valuable

*To whom correspondence should be addressed: Elizabeth Ballou, PhD: e.ballou@exeter.ac.uk Medical Research Council Centre for Medical Mycology at the University of Exeter, Exeter, UK

DOI: 10.1093/infdis/jiae375

potential for diagnosing mucormycosis by enhancing discriminatory detection of Mucorales in tissue.

Keywords: Mucormycosis, invasive fungal infection, monoclonal antibody, fungal cell wall, Mucorales, Fungi

1. INTRODUCTION

Mucormycosis is an aggressive invasive fungal infection (IFI) caused by moulds in the order Mucorales. These are ubiquitous environmental fungi, found globally in soil and on decaying organic matter. Over 20 fungal species within the Mucorales group are known to cause infection in humans, the most common of which is *Rhizopus arrhizus* [1-7]. Whilst considered a rare infection, mucormycosis is the second most common invasive mould infection in children and adults after aspergillosis [8, 9]. The main risk factors are diabetes mellitus, haematological malignancy, and solid organ transplant, yet a wide range of conditions predispose to mucormycosis, including corticosteroid use, neutropoenia, renal failure and deferoxamine therapy [1, 3, 6, 7, 10-12]. Traumatic wounds and burns are common risk factors in otherwise immunocompetent individuals [6, 7, 10, 12]. Incidence is rising globally, likely due to the growing prevalence of diabetes mellitus, increased use of immunosuppressive therapies, and use of azole antifungal prophylaxis in immunosuppressed patients [5, 7, 13-15]. COVID-19 is the most recently identified risk factor and was associated with an unprecedented surge in cases of mucormycosis worldwide, particularly in India where >47,500 cases were reported during a 2-month period in 2021 [2, 4, 16, 17]. Clinical presentation depends on the site of infection, which is most commonly sino-orbital, pulmonary or cutaneous [1, 3, 5, 7, 10]. A consistent feature is aggressive disease with rapid and destructive growth, extensive angioinvasion and subsequent tissue necrosis and infarction. Contiguous spread is common, and haematogenous dissemination occurs in up to 23% of cases [7, 10, 12]. Overall mortality is high, at approximately 50%, and reaches over 90% in disseminated infection [1, 3, 6, 7, 10, 12].

Due to the rising incidence of mucormycosis, consistently high mortality and urgent need for improved diagnostics, Mucorales are ranked as high-priority pathogens by the World Health Organisation (WHO) [18]. Timely diagnosis of invasive infection, allowing prompt and appropriate treatment, is key to improving patient prognosis [19]. Compared to other mycoses, the development of non-culture based diagnostic tools to identify mucormycosis has been neglected. Screening and early diagnosis of IFI in high-risk groups via antigen-based tests that can be performed on blood or other clinical specimens, such as pan-fungal 1-3-β-D-glucan (BDG), *Aspergillus* galactomannan (GM), and Cryptococcal antigen (CrAg), offer important adjuncts to histopathology and culture. However, other than ruling out other IFIs, these are not appropriate for diagnosis of mucormycosis due to the low presence of these antigens in the Mucorales cell wall [17]. Instead, diagnosis continues to rely on histopathology, using non-specific stains to visualise fungal elements in tissue samples, and insensitive culture of fungi

from tissue biopsies or bronchoalveolar lavage fluid (BALf) to confirm identification [17, 20, 21].

Thornton *et al.* recently developed a murine IgG2b monoclonal antibody (mAb), TG11, that is pan-Mucorales specific [22]. TG11 was raised against extracellular polysaccharide (EPS) from *Lichtheimia corymbifera* and binds to EPS antigen secreted by all Mucorales fungi but not unrelated moulds and yeasts including *Aspergillus*, *Candida*, *Cryptococcus*, *Fusarium*, *Lomentospora*, and *Scedosporium* species [22]. TG11 has been incorporated into a lateral flow device to allow the rapid detection of Mucorales from serum or BALf [22], yet the spatio-temporal expression and *in vivo* relevance of this antigen remains undescribed. Here, we investigate the potential of this mAb to differentiate infection from colonisation or sample contamination with environmental spores and to specifically detect invasive disease in murine tissue samples. Specifically, we investigate the dynamics of the antigen recognised by TG11 during spore germination and during invasive growth in tissue, as well as the ability of TG11 mAb to differentiate invasive mucormycosis from invasive aspergillosis, the most relevant clinical differential diagnosis. We characterise the spatio-temporal localisation of the TG11 antigen in the most important causative species of mucormycosis using immunofluorescence and immunogold microscopy. Furthermore, we use an *ex vivo* murine lung infection model to demonstrate the utility of TG11 in visualising invasive hyphal growth in histology sections. Taken together, our work shows that TG11 detects early spore germination and hyphal growth both *in vitro* and in an *ex vivo* murine lung infection model and presents a novel opportunity to detect invasive infections by Mucorales fungi in tissue samples, differentiated from invasive *Aspergillus* infections.

2. MATERIALS AND METHODS

*2.*1 Ethics statement (mouse tissue)

All animal experiments were conducted in compliance with the United Kingdom Home Office licenses for research on animals and approved by the University of Exeter Ethical Review Committee. *Ex vivo* lung infections were performed using uninfected CD1 female mice scheduled to be culled, in keeping with 3Rs objectives to reduce the number of animals involved in research. All experiments were performed at the University of Exeter (establishment license number X7C5DF140).

2.2 Spore harvesting

Fungal spores (Table 1) were cryopreserved at -80^{o}C in YPG broth (0.3% yeast extract, 1% peptone, 2% glucose) containing 50% glycerol and cultured on YPG agar (YPG broth + 2% agar,) 30^{o}C, for 5-7 days, to induce sporulation. *Apophysomyces variabilis* was cultured on Czapek Dox agar (CM0097,Oxoid), 30^{o}C, for 14 days. Spores were harvested from mycelia in 10ml sterile 1xPBS (Oxoid Phosphate Buffered Saline Tablets (Dulbecco A), BR0014G) using

an L-shaped spreader, then spore suspensions were filtered through a 40µm sterile strainer to exclude hyphae, centrifuged (4,000 rpm, 5 min) and supernatants discarded. The pellet was resuspended in 5ml PBS and spores quantified using a Neubauer haemocytometer. Spores were routinely stored at 4 °C for up 14 days.

*2.*3 Cell Preparation, fixation, and staining for indirect immunofluorescence microscopy

The pan-Mucorales-specific monoclonal antibody TG11 and the *Aspergillus*-specific mAb JF5 [24] were gifts from ISCA Diagnostics Limited. Spores were inoculated at 10^7 spores/ml in 5ml HL5 Medium with glucose (HLG0101, Formedium Ltd.) broth and incubated at 37°C (150 rpm) for up to 8 hours. Swollen spores and germlings were pelleted (4,000 rpm for 5 min). For hyphal cultures, cells were collected and pelleted at 13,000 rpm for 5 min. Pellets were washed in 1XPBS (13,000 rpm, 5 min), resuspended in 4% methanol-free formaldehyde in PBS, and incubated on a roller for 1 hour at room temperature (RT). Following incubation, cells were pelleted (13,000 rpm, 5 min), formaldehyde removed, and cells washed twice with 1ml PBS as above. Pellets were resuspended in 1ml 5% bovine serum albumin (BSA) in 0.1%Tween-20 1xPBS (PBST) and incubated on a roller for 30 min, RT. Cells were pelleted at 13,000 rpm, 5 min, and supernatant removed, then resuspended and incubated in 0.5 ml 5 µg/ml TG11 in 1%BSA, 0.1%PBST, 1 hour, RT, on a roller. The cells were pelleted (4,000 rpm, 5 min), antibody solution removed, then washed three times with 1ml PBS. Pellets were incubated (1hr, RT) in 1:1000 Cy5-conjugated goat anti-mouse polyclonal IgG (ab6563; Abcam) (GAM-Cy5) in 1%BSA, 0.1%PBST, with 10µg/ml calcofluor white (CFW), then pelleted (4,000 rpm, 5 min), washed three times with 1ml PBS, and resuspended in 1XPBS. For the germination timeline, *R. arrhizus* var *delemar* spores were inoculated into 17.5ml HL5 broth (37°C, 150 rpm), sampled in 2ml aliquots hourly, then processed as above. Immunoassay controls were performed using *R. arrhizus* var. *delemar* cultured for 4h as described above: positive control with CFW (A+); positive control without CFW (A-); primary only (B); isotype control (C); secondary only with CFW (D+); secondary only without CFW (D-); unstained (E). The isotype control BD6, a murine IgG2b against human Dectin-1 (from Dr. Janet Willment, University of Exeter, UK), was prepared at 5 µg/ml in 1%BSA in 0.1%PBST. Images were acquired using an inverted Deltavision Elite microscope (IMSOL; 60x; DAPI, FITC, Cy5 channels), and acquired as Z-stacks every 0.2 µm for at least 10 µm.

*2.*4 Conjugation of Cy5 to TG11 and BD6

Cy5 was conjugated to TG11 and the BD6 isotype control antibody using Lightning-Link® Rapid Cy5 Antibody labeling kit (AB188288-1003; Bio-techne Ltd., Abingdon, UK). Conjugation was performed as per the manufacturer's instructions, using 0.5 mg/ml antibody.

*2.*5 Direct immunofluorescence time-lapse microscopy of live cells in microfluidic chambers

Spores were inoculated 10^7 spores/ml in YPD and incubated (37°C, 150 rpm) for 2.5 hours to swell, then diluted 1:10 in YPG and loaded into a custom fabricated polydimethylsiloxane (PDMS) microfluidic chamber with U-shaped traps with a height of 10 µm for imaging on a pre-warmed (37°C) inverted Deltavision Elite microscope. The chip was perfused 1µl/min with 1XYNB without amino acids and 3% glucose, 1%BSA, 1µg/ml CFW and 1µg/ml TG11-Cy5,and the cells imaged every 20 minutes for 3 hours.

*2.*6 Immunogold transmission electron microscopy

2.6.1 Conjugation of gold particles to the secondary antibody

Goat anti-mouse polyclonal IgG (ab7063; Abcam) (GAM, 0.1 mg/ml) was directly conjugated to 40 nm gold particles using a gold conjugation kit (ab154873; Abcam) as per the manufacturer's instructions.

2.6.2. Preparation of cells for TEM

R. arrhizus var. *delemar* 99-880 spores were inoculated in 5ml YPG broth at 10^7 spores/ml and incubated at 37°C (150 rpm) for 4 hours, then pelleted as above. Samples were fixed in 4% formaldehyde in cacodylate buffer, then dehydrated in 30, 50, 70, 95 and 100% graded ethanol. After LR (London Resin) White (Agar Scientific, UK) infiltration, samples were polymerized at 60°C in an oxygen free environment. 60 nm sections were mounted on copper grids.

2.6.3 Immunostaining and contrast-staining for TEM

Grids were incubated in a series of 100 µl reagent droplets beaded on parafilm and transferred using a perfect loop. Grids were washed serially with 70% ethanol and sterile deionised water (dH_2O) between transfers. Grids were blocked using 1%BSA, 0.5% Tween 80 in PBS for 20 min, washed three times for 5 min in 0.1% BSA in PBS (incubation buffer), then stained in 5 µg/ml mAb TG11 in incubation buffer for 90 min. (Negative control: incubation buffer alone; IgG2b isotype control: 5 µg/ml BD6 in incubation buffer.) Grids were washed six times for 5 min in incubation buffer, then stained with gold-conjugated goat anti-mouse IgG (50 µl, 1 µg/ml) in incubation buffer for 60 min. Grids were washed 6 times in incubation buffer, three times in PBS, and three times in sterile dH_2O (5 min each). Grids air dried on filter paper, then contrast-stained with a 2% aqueous solution of uranyl acetate for imaging.

2.6.4 Sampling of immuno-gold labelled cells and gold density calculations

Ten images containing cells from a single section from both the TG11 and IgG2b grids were acquired using a systematic random sampling method from the bottom right-hand corner of each grid moving systematically across sections at regular intervals independent of image content at

x3000 magnification. Spore and hyphal cell walls were distinguished visually by the presence of a thickened outer layer. The total number of gold particles detected in the total background area, cell area, and cell walls of spores and hypha were counted as a proxy for TG11 binding. Gold density was calculated by dividing the total area or length of the cell or field (background) by the number of gold particles.

*2.*7 Direct immunofluorescence microscopy of murine lung tissue infected with R. Arrhizus and A. Fumigatus

Female CD1 mice culled by CO_2 inhalation were immediately infected intratracheally with 50 µl PBS containing 10^4 *R. delemar* 99-880 spores, 10^4 *A. fumigatus* A1160p+ spores, or PBS alone. Lungs were harvested and washed in sterile PBS, then incubated for 24 h at 37 ºC and 5% CO_2 in DMEM/F12 medium (Gibco, Ref A4192001), 1% foetal bovine serum (Gibco, Ref A5256801), 1% penicillin/streptomycin (Gibco, 15140-122). Recovered lungs were embedded in OCT medium (Thermo Scientific, Lamb/OCT), fast frozen using dry ice and isopentane and stored at -80 ºC until sectioned via a Leica CM1521 cryostat (Leica bio systems). The 6 µm slices mounted on super-frost glass slides (Epredia Inc, Ref J1800AMNZ) were fixed with 4% methanol-free formaldehyde for 1 h and stored at -20ºC in 70% ethanol in a Coplin jar. For staining, samples were permeabilised using 0.2% Triton x-100 in PBS for 20 min, washed three times with PBS, blocked with 5%BSA in 0.1%PBST for 30 min, then stained with 5 µg/ml TG11-Cy5 conjugate or 5 µg/ml JF5-Cy5 conjugate plus 1x SybrGreen nucleic acid stain (Invitrogen S7563) in 1%BSA in 0.1%PBST and incubated covered in the dark at 4 ºC overnight before counterstaining with 10 µg/ml CFW. Slides were washed with PBS and dried in the dark at RT, then coverslips mounted with 5 µl 90% glycerol in PBS. Infected controls: 1x SybrGreen nucleic acid stain and 10 µg/ml CFW in 1%BSA in 0.1%PBST. Isotype controls: 5 µg/ml Dectin-1/CLEC7A BD6-Cy5 mAb (BioRad MCA4662GA). Images were acquired on a DeltaVison Elite microscope (IMSOL; 60x; DAPI, FITC, Cy5 channels). For *ex vivo* sections, images were acquired every 0.2 µm for 16.8 µm.

*2.*8 Image analysis

All images were analysed using Fiji ImageJ [23]. Germination micrographs and tissue sections are presented as summed Z projections.

3. RESULTS

The TG11 antigen is localised primarily to growing hypha in *R. arrhizus* var. *delemar*

To establish the spatio-temporal localisation of the TG11 antigen, immunofluorescence microscopy was performed on *R. arrhizus* var. *delemar* cells at different stages of growth (Figure 1). Both indirect and direct staining techniques were used to image fixed and live cells respectively. The widely used reference strain *R. arrhizus* var. *delemar* 99-880 was imaged for

these experiments as *R. arrhizus* is the single most common causative species of mucormycosis. There was no binding of mAb TG11 to ungerminated spores (data not shown). Fixed cells collected hourly after spores were allowed to swell for 2 hours showed TG11 staining at the site of polarisation (3hrs), on the emerging germ tube (4-6hrs), and localised to hyphae (6-7hrs) (Figure 1A). Live imaging of spores pre-germinated for 2.5 hrs revealed that TG11 antigen is first detectable at the tip of the emerging germ tube and then remains detectable along the whole length of the developing hypha (Figure 1B and Supplemental movie 1). Negative controls lacking the primary TG11 mAb showed the absence of non-specific staining by the secondary antibody (GAM-Cy5) (Figure 1 Ci) and no change in TG11 binding in the absence of the chitin-binding dye calcofluor white (CFW) (Figure 1 Cii).

The TG11 antigen is detectable on the hyphal surface of Rhizopus, Mucor, Lichtheimia, Cunninghamella, Apophysomyces, Rhizomucor, Saksenaea and Syncephalastrum isolates.

Indirect immunofluorescence microscopy was performed on an additional ten different mucoralean fungi (Table 1). The TG11 antigen was detected in all ten isolates (Figure 2).

Whilst TG11 localised to the fungal hyphae, there were some notable differences in antigen distribution in some isolates. *R. arrhizus* var. *arrhizus*, *Rhizopus microsporus*, *Mucor circinelloides*, *Lichtheimia corymbifera*, *Cunninghamella bertholletiae*, *Apophysomyces variabilis* and *Rhizomucor pusillus* had a similar staining pattern to that of *R. arrhizus* var. *delemar*, with homogenous staining along the length of the hyphae and sparingly of the spore body (figure 2a-d,f-h). Similarly, staining of *Saksenaea erythrospora* was predominantly located to the hyphae and sparingly of the spore body, however in cells with longer hyphae it was apparent that staining did not extend along the whole length of the hyphae, but remained localised to the proximal part (Figure 2i). Both *Lichtheimia ramosa* (Figure 2e) and *Syncephalastrum contaminatum*. (Figure 2j) exhibited a more punctate staining pattern, with some variable staining of the spore body. In addition, ungerminated *S. contaminatum* spores were observed to exhibit variable morphology, including larger rounded cells that stained with both TG11 and CFW, elongated cells that stained with TG11 but not CFW, and small rounded cells that stained with CFW but not TG11 (Figure 2i). This suggests species-specific differences in the distribution and exposure of this otherwise hyphal-associated antigen.

The TG11 antigen is localized to the fungal cell wall in both germinating spore and hyphae

Together, these observations suggested that TG11 is a cell-wall-associated antigen that is enriched in Mucorales hypha. To gain a more detailed understanding of the location and abundance of the TG11 antigen, the sub-cellular localisation of immunogold labelled mAb TG11 was visualised in *R. arrhizus* var. *delemar* by TEM (Figure 3).

Consistent with enrichment of fluorescent signal along the growing hypha (Figure 1), more gold particles were observed in the hyphal cell wall than in the spore cell wall (Figure 3A,B). The TG11-specific gold density of the hyphal cell wall was 3.96 per μm^2 (isotype control 0.0548 per

um^2), while the density was 2.71 per µm^2 in the spore body cell wall (isotype control 0.0606 per µm^2). In addition, an enrichment of gold particles was observed within the cytoplasm of germinating spores (Figure 3C), indicative of trafficking of the target antigen within the cell. There was limited non-specific background and isotype controls (Figure 3D). The gold density of the total cell area was 9.94 per µm^2 for the TG11-stained cells compared to 0.134 per µm^2 for the isotype control and 0.0342 per µm^2 for the background of the TG11-stained section. This was comparable to isotype control background particle density of 0.0420 per µm^2. Both the hyphal wall and cytoplasmic localisation are consistent with previous identification of the TG11 antigen as a secreted polysaccharide [22].

The TG11 antigen is detectable in hyphae in an *ex vivo* lung infection model

To investigate the suitability of mAb TG11 for identification of Mucorales infections in histology sections, murine lungs were infected *ex vivo* with 10^4 *R. arrhizus* var. *delemar* 99-880 spores or *A. fumigatus* A1160p+ spores. After 24 hours, infected lungs were fixed and sectioned, then stained for epifluorescence microscopy. Fungal hyphae were clearly visible within murine airways by CFW staining. Consistent with *in vitro* staining, the TG11 antigen was observed along the length of the growing *R. arrhizus* hypha but not *A. fumigatus* hyphae, which was instead detected by an *Aspergillus*-specific mAb JF5 (Figure 4) [24].

3. DISCUSSION

Here we demonstrate, using immunofluorescence and immunogold electron microscopy, that mAb TG11 detects both early and later stage hyphal growth of eleven different Mucorales fungi. We imaged *R. arrhizus* var. *delemar* at different stages of development both fixed and over time and showed the TG11 antigen is first detectable polarised to the emerging germ tube and then along the length of the extending hypha. Furthermore, the TG11 antigen is detectable in *ex vivo* murine lung tissue following invasive infection, and the TG11 mAb is able to differentiate invasive disease caused by Mucorales versus *Aspergillus* species, consistent with previous work demonstrating the specificity of the TG11 mAb for Mucorales fungi [19].

Mucormycosis is caused by a diverse group of over 20 different fungal species [1-7]. Our study demonstrated that the TG11 antigen is reliably produced by the eleven most common causative species of mucormycosis: *Rhizopus arrhizus* var. *delemar*, *Rhizopus arrhizus* var. *arrhizus*, *Rhizopus microsporus*, *Mucor circinelloides*, *Lichtheimia corymbifera*, *Lichtheimia ramosa*, *Cunninghamella bertholletiae*, *Apophysomyces variabilis*, *Rhizomucor pusillus*, *Saksenaea erythrospora* and *Syncephalastrum contaminatum*. The mAb TG11 predominantly bound to hypha, and immunogold-TG11 TEM of *R. arrhizus* var. *delemar* revealed abundant antigen in the hyphal cell wall of germinated spores. Together, these results demonstrate the ability of mAb TG11 to detect invasive hyphal growth specifically of Mucoralean fungi.

The pathogenesis of mucormycosis is best understood for *R. arrhizus*. Infection occurs via inhalation, traumatic inoculation, or contamination of wounds. If not cleared by the immune system, spore germination is followed by hyphal growth, angioinvasion, and tissue necrosis [25, 26]. A biomarker for invasive hypha may reflect fungal burden and invasive disease. The majority of Mucorales species imaged exhibited similar staining patterns to *R. arrhizus* var. *delemar*, with sparse staining of spores and homogenous staining along hyphae. Antigen production may therefore correlate well with burden of hyphal growth and invasive disease.

Mucorales are ubiquitous environmental organisms and their spores can colonise human sinuses, upper respiratory tract and skin without causing invasive disease [27, 28]. An ideal diagnostic antigen for mucormycosis should differentiate invasive hyphal growth from host colonisation or environmental contamination of the clinical sample. The mAb TG11 allows actively germinating spores that produce invasive hyphae to be distinguished from dormant, ungerminated spores. Whilst this may not be possible for all fungi, such as *Syncephalastrum contaminatum*, where mAb TG11 stained elongated spores, our data demonstrate it is possible for the most important agents of mucormycosis, *Rhizopus* spp., *Mucor* spp. and *Lichtheimia* spp. Further studies are required to understand the clinical significance of this elongated *S. contaminatum* spore morphology, including whether these spores can germinate and cause invasive infection *in vivo*. In the *ex vivo* murine lung tissue infection model, TG11 detected invasive *R. arrhizus* var. *delemar* hyphae. This experiment demonstrates that the fungus produces the TG11 antigen in physiologically relevant growth conditions and in the presence of murine airway immune cells. TG11 may therefore have potential as an immunohistochemistry stain to enhance the detection of mucormycosis in histology samples, and to differentiate Mucorales infections from those caused by other fungi such as *Aspergillus fumigatus*, the most common mould pathogen of humans.

CONCLUSIONS

The antigen recognised by mAb TG11 is, to our knowledge, the first potential pan-Mucorales-specific antigen for active Mucorales growth. The next step in evaluating the potential of mAb TG11 for diagnosing mucormycosis should focus on its ability to detect the TG11 antigen in more easy accessible clinical samples such as serum and urine to facilitate an earlier diagnosis.

Acknowledgements: We thank Dr Christian Hacker and Dr Lenka Koptasikova at the Exeter University Bioimaging Centre and Mrs Gillian Milne and the Microscopy & Histology Facility, University of Aberdeen, for help with TEM sample preparation and imaging. We acknowledge the patients and Professors Andrew Borman and Elizabeth Johnson at the UK Health Security Agency National Collection of Pathogenic Fungi, Bristol, UK for providing clinical isolates. We gratefully acknowledge our funders. AH is supported by Noah's Pink Balloon Leukaemia Fund. DECL and ERB are jointly supported by the UK Biotechnology and Biological Sciences Research Council and the USA National Science Foundation (BB/W002760/1). IK and DW are funded by a

Wellcome Trust Senior Research Fellowship (214317/Z/18/Z). ERB is supported by a Sir Henry Dale Fellowship jointly funded by the Wellcome Trust and the Royal Society (211241/Z/18/Z) and the Lister Institute. AH, DECL, IK, DW, AW and ERB are supported by the Medical Research Council Centre for Medical Mycology (MR/N006364/2). This study was supported by the NIHR Exeter Biomedical Research Centre. Additional work may have been undertaken by the University of Exeter Biological Services Unit. The views expressed are those of the author(s) and not necessarily those of the NIHR or the Department of Health and Social Care.

Conflict of interest: CRT is a Director of ISCA Diagnostics Limited. The funders had no role in study design, data collection and interpretation, or the decision to submit the work for publication.

Author Contributions: AH, DECL, AW, ERB Conceptualization; AH, DECL IK, ERB Investigation, Validation, Data Curation, Visualization, Formal analysis; AH, DECL, ERB Writing - Original Draft; AH, DECL, IK, DW, CT, AW, ERB Writing - Review & Editing; DW, CT, AW, ERB Resources, Supervision, Funding Acquisition

Footnote page:

Conflict of interest: CRT is a Director of ISCA Diagnostics Limited. The funders had no role in study design, data collection and interpretation, or the decision to submit the work for publication.

Funding statement; We gratefully acknowledge our funders. AH is supported by Noah's Pink Balloon Leukaemia Fund. DECL and ERB are jointly supported by the UK Biotechnology and Biological Sciences Research Council and the USA National Science Foundation (BB/W002760/1). IK and DW are funded by a Wellcome Trust Senior Research Fellowship (214317/Z/18/Z). ERB is supported by a Sir Henry Dale Fellowship jointly funded by the Wellcome Trust and the Royal Society (211241/Z/18/Z) and the Lister Institute. AH, DECL, IK, DW, AW and ERB are supported by the Medical Research Council Centre for Medical Mycology (MR/N006364/2). This study was supported by the NIHR Exeter Biomedical Research Centre. Additional work may have been undertaken by the University of Exeter Biological Services Unit. The views expressed are those of the author(s) and not necessarily those of the NIHR or the Department of Health and Social Care.

Meeting statement: The information presented in this manuscript has been previously presented at the British Society for Medical Mycology Annual Meeting (2023), the 2024 Keystone Symposium on Fungal Pathogens: Emerging Threats and Future Challenges, and ECMID 2024.

To whom correspondence should be addressed: Elizabeth Ballou, PhD: e.ballou@exeter.ac.uk

Medical Research Council Centre for Medical Mycology at the University of Exeter, Exeter, UK

References

1. Corzo-Leon, D.E., et al., Diabetes mellitus as the major risk factor for mucormycosis in Mexico: Epidemiology, diagnosis, and outcomes of reported cases. Med Mycol, 2018. **56**(1): p. 29-43.
2. Hoenigl, M., et al., The emergence of COVID-19 associated mucormycosis: a review of cases from 18 countries. Lancet Microbe, 2022. **3**(7): p. e543-e552.
3. Osaigbovo, II, et al., Mucormycosis in Africa: Epidemiology, diagnosis and treatment outcomes. Mycoses, 2023. **66**(7): p. 555-562.
4. Ozbek, L., et al., COVID-19-associated mucormycosis: a systematic review and meta-analysis of 958 cases. Clin Microbiol Infect, 2023. **29**(6): p. 722-731.
5. Prakash, H. and A. Chakrabarti, Global Epidemiology of Mucormycosis. J Fungi (Basel), 2019. **5**(1).
6. Prakash, H., et al., A prospective multicenter study on mucormycosis in India: Epidemiology, diagnosis, and treatment. Med Mycol, 2019. **57**(4): p. 395-402.
7. Roden, M.M., et al., Epidemiology and outcome of zygomycosis: a review of 929 reported cases. Clin Infect Dis, 2005. **41**(5): p. 634-53.
8. Francis, J.R., et al., Mucormycosis in Children: Review and Recommendations for Management. J Pediatric Infect Dis Soc, 2018. **7**(2): p. 159-164.
9. Thornton, C.R., Detection of the 'Big Five' mold killers of humans: Aspergillus, Fusarium, Lomentospora, Scedosporium and Mucormycetes. Adv Appl Microbiol, 2020. **110**: p. 1-61.
10. Jeong, W., et al., The epidemiology and clinical manifestations of mucormycosis: a systematic review and meta-analysis of case reports. Clin Microbiol Infect, 2019. **25**(1): p. 26-34.
11. Prakash, H. and A. Chakrabarti, Epidemiology of Mucormycosis in India. Microorganisms, 2021. **9**(3).
12. Skiada, A., et al., Zygomycosis in Europe: analysis of 230 cases accrued by the registry of the European Confederation of Medical Mycology (ECMM) Working Group on Zygomycosis between 2005 and 2007. Clin Microbiol Infect, 2011. **17**(12): p. 1859-67.
13. Bitar, D., et al., Population-based analysis of invasive fungal infections, France, 2001-2010. Emerg Infect Dis, 2014. **20**(7): p. 1149-55.
14. Kontoyiannis, D.P., et al., Zygomycosis in a tertiary-care cancer center in the era of Aspergillus-active antifungal therapy: a case-control observational study of 27 recent cases. J Infect Dis, 2005. **191**(8): p. 1350-60.
15. Pongas, G.N., et al., Voriconazole-associated zygomycosis: a significant consequence of evolving antifungal prophylaxis and immunosuppression practices? Clin Microbiol Infect, 2009. **15 Suppl 5**: p. 93-7.
16. Hoenigl, M., et al., COVID-19-associated fungal infections. Nat Microbiol, 2022. **7**(8): p. 1127-1140.
17. Pham, D., et al., Epidemiology, Modern Diagnostics, and the Management of Mucorales Infections. J Fungi (Basel), 2023. **9**(6).
18. World Health Organisation. WHO fungal priority pathogens list to guide research, development and public health action. WHO, 2022.
19. Chamilos, G., R.E. Lewis, and D.P. Kontoyiannis, Delaying amphotericin B-based frontline therapy significantly increases mortality among patients with hematologic malignancy who have zygomycosis. Clin Infect Dis, 2008. **47**(4): p. 503-9.

20. Lass-Florl, C., Zygomycosis: conventional laboratory diagnosis. Clin Microbiol Infect, 2009. **15 Suppl 5**: p. 60-5.
21. Skiada, A., I. Pavleas, and M. Drogari-Apiranthitou, Epidemiology and Diagnosis of Mucormycosis: An Update. J Fungi (Basel), 2020. **6**(4).
22. Thornton, C.R., G.E. Davies, and L. Dougherty, Development of a monoclonal antibody and a lateral-flow device for the rapid detection of a Mucorales-specific biomarker. Front Cell Infect Microbiol, 2023. **13**: p. 1305662.
23. Schindelin, J., et al., Fiji: an open-source platform for biological-image analysis. Nat Methods, 2012. **9**(7): p. 676-82.
24. Davies G, et al., Towards Translational ImmunoPET/MR Imaging of Invasive Pulmonary Aspergillosis: The Humanised Monoclonal Antibody JF5 Detects Aspergillus Lung Infections In Vivo. . Theranostics, 2017. **11**(14): p. 3398-3414.
25. Corzo-Leon, D.E., J.K. Uehling, and E.R. Ballou, Rhizopus arrhizus. Trends Microbiol, 2023. **31**(9): p. 985-987.
26. Ibrahim, A.S., et al., Pathogenesis of mucormycosis. Clin Infect Dis, 2012. **54 Suppl 1**(Suppl 1): p. S16-22.
27. Ambrosioni, J., K. Bouchuiguir-Wafa, and J. Garbino, Emerging invasive zygomycosis in a tertiary care center: epidemiology and associated risk factors. Int J Infect Dis, 2010. **14 Suppl 3**: p. e100-3.
28. Langford, S., et al., Mucormycete infection or colonisation: experience of an Australian tertiary referral centre. Mycoses, 2016. **59**(5): p. 291-5.
29. Ma, L.J., et al., Genomic analysis of the basal lineage fungus Rhizopus oryzae reveals a whole-genome duplication. PLoS Genet, 2009. **5**(7): p. e1000549.
30. Itabangi, H., et al., A bacterial endosymbiont of the fungus Rhizopus microsporus drives phagocyte evasion and opportunistic virulence. Curr Biol, 2022. **32**(5): p. 1115-1130 e6.
31. Marcin G. Fraczek, et al., The cdr1B efflux transporter is associated with non-cyp51a-mediated itraconazole resistance in Aspergillus fumigatus. Journal of Antimicrobial Chemotherapy, 2013. **68**(7): p. 1486–1496.
32. Margherita Bertuzzi, et al., On the lineage of Aspergillus fumigatus isolates in common laboratory use. Medical Mycology, 2021. **59**(1): p. 7-13.

FIGURE LEGENDS

Figure 1. *R. arrhizus* var. *delemar* cells immunostained with mAb TG11 at different stages of spore swelling, germination and hyphal growth. A. Composite photomicrographs and individual channels of *R. arrhizus* strain 99-880 using DAPI (for CFW) and Cy5 (for TG11+ GAM-Cy5) filters. Cells are stained with mAb TG11 plus Cy5-conjugated goat anti-mouse polyclonal IgG (GAM-Cy5) (orange), and CFW (blue). Representative cells from liquid culture after 2h, 3h, 4h, 5h, 6h and 7h of incubation were imaged to visualise binding by mAb TG11 at different stages of cell growth. B. Time-lapse image series of a single live *R. arrhizus* cell grown in media containing CFW and TG11-Cy5 and collected every 20 minutes. Note that indicated times are from the start of imaging with spores pre-germinated for 2.5hrs. TG11 is seen to stain the growing hypha (yellow). C. Representative negative controls i. CFW, secondary only; ii. no CFW, TG11 + goat anti-mouse polyclonal IgG (GAM-Cy5). Scale bars = 20 μm.

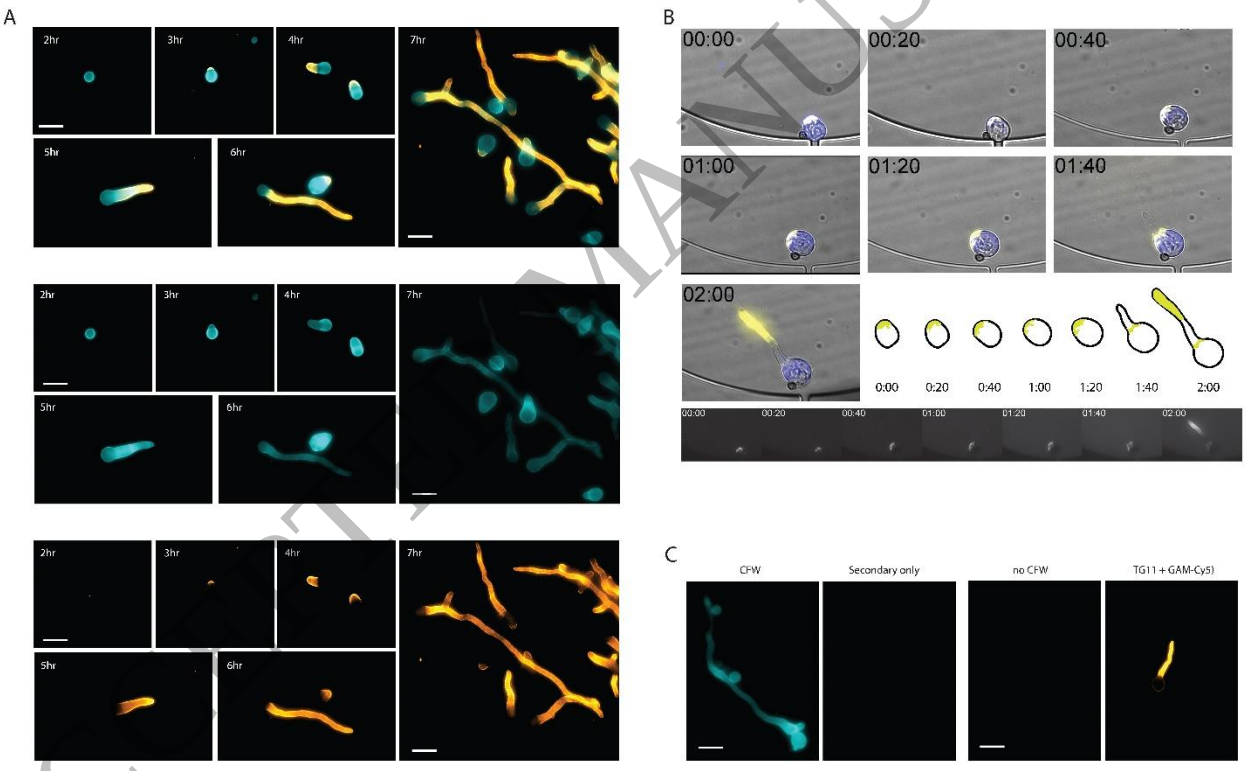

Figure 2. Different mucoralean fungi immunostained with mAb TG11.

Composite photomicrographs of (a) R. arrhizus var. arrhizus MRL 21E307, (b) Rhizopus microsporus FP469-12, (c) Mucor circinelloides MRL 22E56177, (d) Lichtheimia corymbifera MRL 20E42327, (e) Lichtheimia ramosa MRL 21E1059, (f) Cunninghamella bertholletiae CBS151.80, (g) Apophysomyces variabilis CBS658.93, (h) Rhizomucor pusillus MRL 22E19013, (i) Saksenaea erythrospora CBS138.279 and (j) Syncephalastrum contaminatum MRL 22E22635 taken with DAPI and Cy5 fluorescence filters. Cells are stained with mAb TG11 plus Cy5-conjugated goat anti-mouse polyclonal IgG (GAM-Cy5) (orange), and CFW (blue).

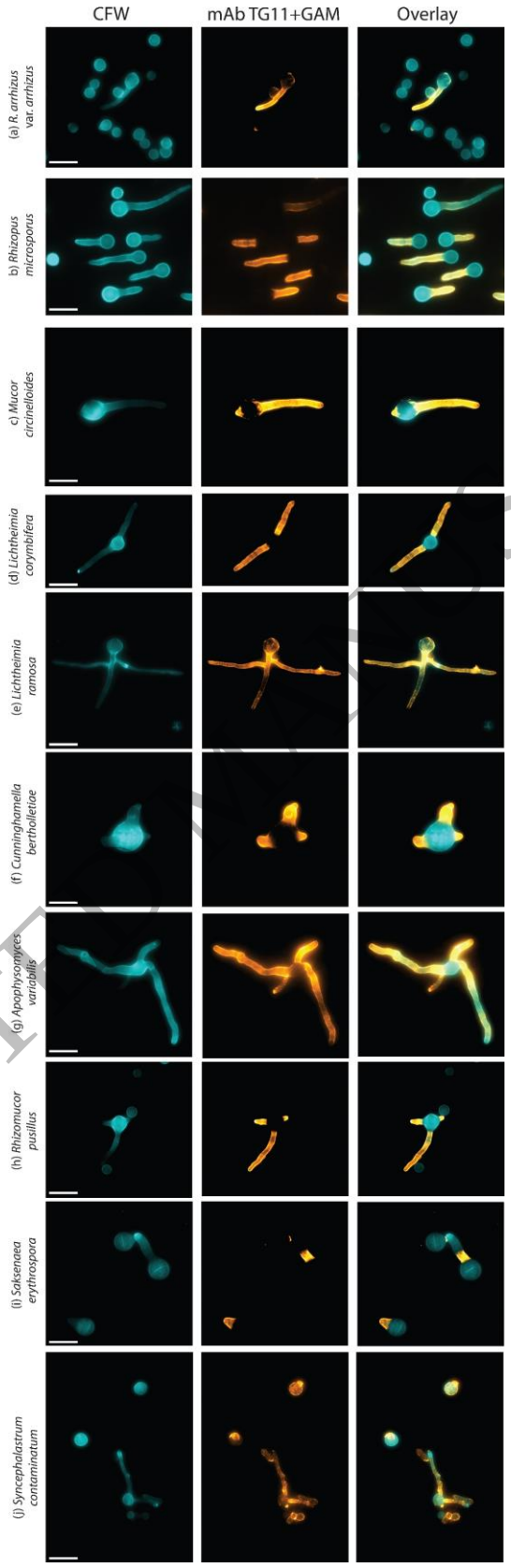

Figure 3. Transmission electron microscopy of immunogold-labelled R. arrhizus var. delemar. TEM images of R. arrhizus var. delemar stained with (A,B,C) TG11 or (D) an IgG2b isotype control, and a gold-conjugated secondary antibody. Gold particles are predominantly localised to the hyphal cell wall (B) as well as to the cytoplasm of germinating spores (C). Panels B and C show higher magnifications of the region identified in panel A by white squares. Note that panel C represents an independent slice of cells imaged in panel A.

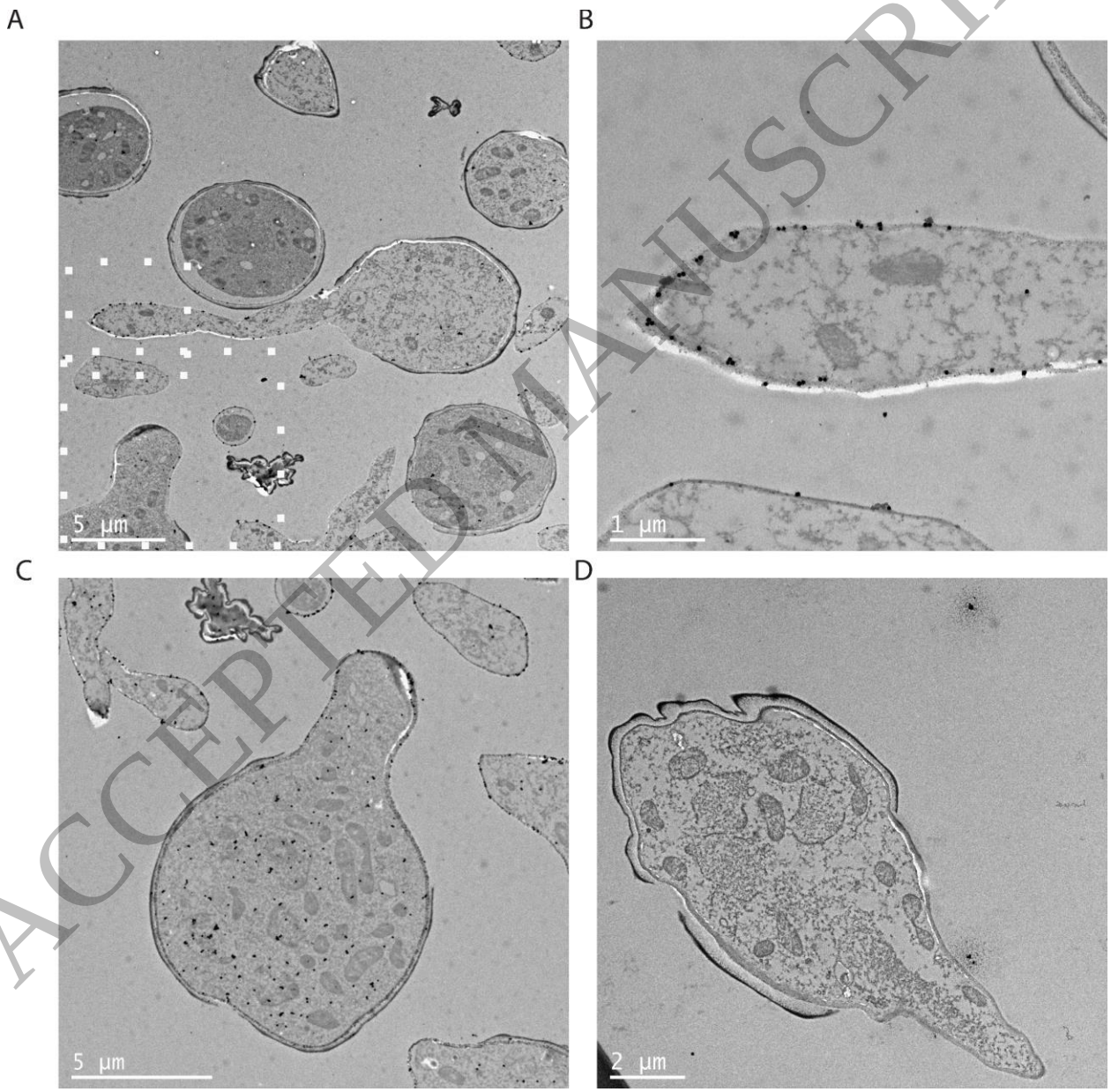

Figure 4. Ex vivo murine lung tissue infected with R. arrhizus var. delemar and immunostained with mAb TG11. Photomicrographs of murine lung tissue uninfected (first row only) or infected with R. arrhizus strain 99-880 or A. fumigatus strain A1160^{+}. Images were acquired with DAPI (CFW), Cy5 (mAb TG11-GAM; mAb JF5-GAM) and FITC (SybrGreen) fluorescence filters. Tissue slices are stained with (first, second, fifth rows) mAb TG11 plus GAM-Cy5 (magenta), (sixth, seventh rows) mAb JF5 plus GAM-Cy5 (magenta); (third row) IgG2b isotype control plus GAM, (fourth row) no primary +GAM alone, CFW for fungal chitin (blue) and Sybrgreen for DNA to reveal host cell nuclei (yellow). Note that lung connective tissue and alveolae also stain with CFW but not with mAb TG11-GAM or mAb JF5-GAM. Isotype control is a representative image for both conjugated antibodies. Images acquired in z-stack every 0.2 µm are presented as summed z- projections. Scale bars indicate 10 µm.

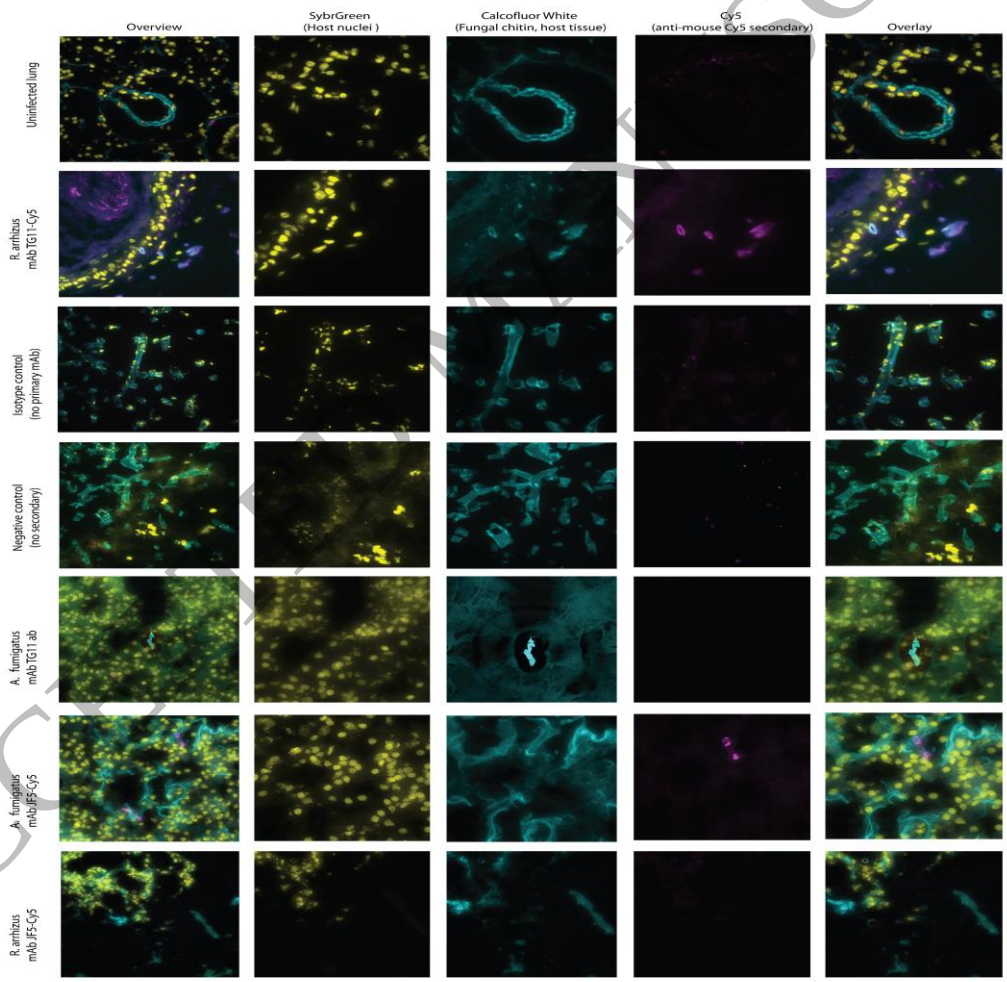

Table 1. Details of mucoralean fungal strains used in this study. Species are listed in order of the frequency with which they are isolated from clinical cases of mucormycosis [1-7].

Species	Isolate number	Origin	Source
Rhizopus arrhizus var. *delemar*	RA 99-880	Reference strain[1]	ATCC
Rhizopus arrhizus var. *arrhizus*	MRL 21E307	Clinical isolate	UKHSA
Rhizopus microsporus	FP469-12	Clinical isolate[2]	QEHB
Mucor circinelloides	MRL 22E56177	Clinical isolate	UKHSA
Lichtheimia corymbifera	MRL 20E42327	Clinical isolate	UKHSA
Lichtheimia ramosa	MRL 21E1059	Clinical isolate	UKHSA
Cunninghamella bertholletiae	CBS 151.80	Clinical isolate	CBS
Apophysomyces variabilis	CBS 658.93	Clinical isolate	CBS
Rhizomucor pusillus	MRL 22E19013	Clinical isolate	UKHSA
Saksenaea erythrospora	CBS 138279	Clinical isolate	CBS
Syncephalastrum contaminatum	MRL 22E22635	Clinical isolate	UKHSA
Aspergillus fumigatus	A1160^{+}	Clinical isolate[3]	FGSC

1Strain RA 99-880 was originally a clinical isolate, from Ma *et al*. 2009 [29], and is a widely used reference strain. ATCC; American Type Culture Collection. 2Strain FP469-12 is a clinical isolate from Itabangi *et al*. 2020 [30]. 3Strain A1160+ was derived from a clinical isolate, from Fraczek et al., 2013[31, 32]. QEHB; Queen Elizabeth Hospital, Birmingham. Isolated by Deborah Mortiboy. CBS; Westerdijk Fungal Biodiversity Institute, The Netherlands. UKHSA; UK Health Security Agency National Collection of Pathogenic Fungi, Bristol, UK. FGSC: Fungal Genetics Stock Centre, KY, USA.